Diagn Interv Radiol 2019; 25: 5–13

ABDOMINAL IMAGING

ORIGINAL ARTICLE

Discrimination of oncocytoma and chromophobe renal cell carcinoma using MRI

Işıl Başara Akın
Canan Altay
Ezgi Güler
İlkay Çamlıdağ
Mustafa Harman
Murat Danacı
Burçin Tuna
Kutsal Yörükoğlu
Mustafa Seçil

PURPOSE
We aimed to evaluate magnetic resonance imaging (MRI) features, including signal intensities, enhancement patterns and T2 signal intensity ratios to differentiate oncocytoma from chromophobe renal cell carcinoma (RCC).

METHODS
This retrospective study included 17 patients with oncocytoma and 33 patients with chromophobe RCC who underwent dynamic MRI. Two radiologists independently reviewed images blinded to pathology. Morphologic characteristics, T1 and T2 signal intensities were reviewed. T2 signal intensities, wash-in, wash-out values, T2 signal intensity ratios were calculated. Sensitivity and specificity analyses were performed.

RESULTS
Mean ages of patients with oncocytoma and chromophobe RCC were 61.0±11.6 and 58.5±14.0 years, respectively. Mean tumor size was 60.6±47.3 mm for oncocytoma, 61.7±45.9 mm for chromophobe RCC. Qualitative imaging findings in conventional MRI have no distinctive feature in discrimination of two tumors. Regarding signal intensity ratios, oncocytomas were higher than chromophobe RCCs. Renal oncocytomas showed higher signal intensity ratios and wash-in values than chromophobe RCCs in all phases. Fast spin-echo T2 signal intensities were higher in oncocytomas than chromophobe RCCs.

CONCLUSION
Signal intensity ratios, fast spin-echo T2 signal intensities and wash-in values constitute diagnostic parameters for discriminating between oncoytomas and chromophobes. In the excretory phase of dynamic enhanced images, oncocytomas have higher signal intensity ratio than chromophobe RCC and high wash-in values strongly imply a diagnosis of renal oncocytoma.

Adult renal tumors have been classified into various types by the World Health Organization (1). Among them, renal oncocytoma and chromophobe renal cell carcinoma (RCC) originate from intercalated cells in the collecting duct and share some morphologic, histologic, electron microscopy findings, and immunohistochemical characteristics (2, 3). Although they have common pathologic features, renal oncocytomas are benign, whereas chromophobe RCCs are malignant. Chromophobe RCC constitutes approximately 6%–8% of all renal tumors and approximately 4%–10% of all cases of RCC (4, 5). Oncocytoma is the second most frequent benign renal parenchymal tumor, accounting for 3%–7% of all renal lesions (6).

So far preoperative differentiation between oncocytomas and chromophobe RCCs could not be done accurately using imaging methods, and both tumor types have been treated surgically. Avoidance of surgery, or application of a nephron-sparing approach for benign lesions, has been an important topic for imaging studies in recent years. Some of these studies have involved computed tomography (7–13), and others magnetic resonance imaging (MRI) (12, 13).

In this study, we investigated the MRI features of renal tumors, namely T2 signal intensities, T2 signal intensity ratios, enhancement patterns, and enhancement ratios that might allow differentiation of oncocytoma from chromophobe RCC.

From the Departments of Radiology (I.B.A. ✉ *isilbasara@gmail.com*, C.A., M.S.) and Pathology (B.T., K.Y.), Dokuz Eylül University School of Medicine, İzmir, Turkey; Department of Radiology (E.G., M.H.) Ege University School of Medicine, İzmir, Turkey; Department of Radiology (İ.Ç., M.D.), Ondokuz Mayıs University School of Medicine, Samsun, Turkey.

Received 17 January 2018; revision requested 13 March 2018; last revision received 30 May 2018; accepted 19 June 2018.

DOI 10.5152/dir.2018.18013

You may cite this article as: Başara Akın I, Altay C, Güler E, et al. Discrimination of oncocytoma and chromophobe renal cell carcinoma using MRI. Diagn Interv Radiol 2019; 25: 5–13.

Table 1. MRI examination protocols

Parameter	MRI sequences				
	Fast spin-echo T2-weighted	Fat-saturated T2-weighted	T1-weighted[a]	Dynamic[b]	Late post-contrast
Plane	Axial	Axial/coronal	Axial	Axial	Coronal
Fat saturation	+	-	-	+	+
TR/TE	2400–3260/70–101	1312/325	196/4.6 in-phase 253/6.9 opposed phase	272/6.9	272/6.9
Flip angle (°)	90	90	80 in/opposed phase	70	70
Slice thickness (mm)	5–8	5–8	5–8 in/opposed phase	4.5–5	5–6
FOV (mm^2)	400–445	435–445	435–445 in/opposed phase	435–445	435–445
Scan time (s)	300	180	120	300	80
Delay (s)	-	-	-	0, 40, 100, 220	-

MRI, magnetic resonance imaging; TR, repetition time; TE, echo time; FOV, field of view.
[a]Scanner 1 and 2, FFE; scanner 3–5, FLASH 2D.
[b]Scanner 1 and 2, THRIVE-WATS; scanner 3 and 5, FLASH 3D; scanner 4, VIBE.

Methods

Patients

The institutional review board approved this multicenter retrospective study. The requirement for informed consent was waived due to the retrospective nature of the study. (The protocol number of non-interventional investigation ethical committee approval was 3476 and decision number was 2017/25-30). The databases of three institutions, covering the period from June 2009 to December 2015, were reviewed to identify MRI data of patients with a histopathologic diagnosis of oncocytoma or chromophobe RCC. Total number of patients reviewed in the study was 61, with 37 patients diagnosed as chromophobe RCC and 24 patients diagnosed with oncocytoma. Fifty patients who were examined with appropriate MRI technique without missing data and received final histopathologic diagnoses via surgery including either total or subtotal nephrectomy were included in the study. Eight patients with missing, inadequate or inappropriate MRI data were excluded from the study. As the core biopsy diagnosis of oncocytoma is a debated subject among pathologists (14), we preferred to exclude 3 patients who received diagnosis with core needle biopsy.

Main points

- Morphologic MRI features cannot be used to distinguish renal oncocytomas from chromophobe RCCs.
- Signal intensity ratios constitute a radiologic diagnostic parameter for discriminating between renal oncocytomas and chromophobe RCCs.
- A high wash-in value strongly indicates a diagnosis of renal oncocytoma.
- As the treatment options for these tumors are different, dynamic MRI sequences and signal intensity measurements could facilitate correct diagnosis and management.

MRI techniques

All MRI examinations were carried out with four clinical 1.5 T systems (Intera, [software version 8.1], Philips Medical Systems; Gyroscan Achieva, Philips Medical Systems; Vision, Siemens; and Magnetom, Siemens Symphony Quantum) and one 3 T system (Magnetom Verio, Siemens), with the use of phased-array coils. All examination parameters were similar. The examination protocols are shown in Table 1.

Fat-saturated, T1-weighted multiphasic contrast-enhanced dynamic series were obtained both immediately before and during rapid bolus intravenous injection of 0.1 mmol/kg (0.5 mmol/mL) gadopentetate dimeglumine per kilogram of body weight, while the patient was in the bore of the magnet, followed by a 20 mL saline flush. Subtraction of the multiphasic contrast-enhanced dynamic series was performed automatically by the imaging software. The dynamic series included precontrast, arterial, parenchymal, and excretory phase images of the kidney. The arterial phase was determined as the time to peak enhancement of the abdominal aorta at the level of the renal arteries. Acquisition in the arterial, parenchymal and excretory phases began at 32–40, 100, and 200 seconds after the start of acquisition, respectively.

Qualitative and quantitative image analysis

All images were reviewed by two radiologists, one with 12 years and one with 16 years of abdominal radiology experience. Both reviewers were aware that the renal tumors could only be oncocytoma or chromophobe RCC, but they were blind to the final histopathologic diagnosis. The morphologic characteristics of the tumors were evaluated, including the size, growth pattern (exophytic/endophytic), and T1 and T2 signal intensities of the tumor and central scar (if present). The MRI signal intensities of the tumors were compared with those of the renal parenchyma and categorized as hyper-, iso- or hypointense relative to the renal parenchyma. Tumor homogeneity or heterogeneity was noted. Tumors including areas with different signal intensities were noted as heterogeneous; other tumors were noted as homogeneous. For each tumor, the radius, exophytic/endophytic properties, nearness of tumor to the collecting system or sinus in millimeters, anterior/posterior, location relative to polar

lines (RENAL) nephrometry score was calculated (15).

The signal intensity ratios of tumors on both T2-weighted images were calculated to quantitatively evaluate the tumor intensities. Identical regions of interest (ROIs) were placed on the tumor and kidneys, on both the ipsilateral and contralateral sides. The sizes of ROI were 10–100 mm. All ROIs were appropriate for each tumor and measured part of kidney. ROIs were placed in axial images and the most enhancing portion of the tumor. The equation used for this calculation was:

$$Signal\ intensity\ ratio = (SI_{tumor} / SI_{ipsilateral\ kidney}) \times 100$$
$$Signal\ intensity\ ratio = (SI_{tumor} / SI_{contralateral\ kidney}) \times 100$$

Enhancement of tumors was quantitatively analyzed using pre- and postcontrast dynamic T1-weighted fat-saturated multiphasic dynamic series (arterial, parenchymal and excretory phases). ROIs were drawn on the abdominal aorta at the level of the renal arteries, renal cortex on the tumor site, solid and enhancing component of each tumor, and extraabdominal noise area. Extraabdominal noise was calculated in order to standardize other signal intensities. Cystic components and sites of tumor hemorrhage and necrosis were excluded from the ROIs. To eliminate variation in contrast material relaxivity among patients, institutions and MRI machines, the signal intensity ratios were calculated using the formulas below:

$$Arterial\ phase\ signal\ intensity\ ratio = (Post\text{-}contrast\ SI_{arterial} - Pre\text{-}contrast\ SI) / Post\text{-}contrast\ SI_{arterial} \times 100$$
$$Parenchymal\ phase\ signal\ intensity\ ratio = (Post\text{-}contrast\ SI_{parenchymal} - Pre\text{-}contrast\ SI) / Post\text{-}contrast\ SI_{parenchymal} \times 100$$
$$Excretory\ phase\ signal\ intensity\ ratio = (Post\text{-}contrast\ SI_{excretory} - Pre\text{-}contrast\ SI) / Post\text{-}contrast\ SI_{excretory} \times 100$$

Where SI is the signal intensity values of the arterial, parenchymal or excretory phase.

Tumor wash-in and wash out values were also calculated:

$$Wash\text{-}in = (SI_{enhanced} - SI_{unenhanced}) / SI_{unenhanced} \times 100$$

Three different wash-in values, for the early arterial contrast-enhanced arterial phase, parenchymal phase, and excretory phase, were obtained.

Parenchymal phase wash-out was also calculated:

$$Wash\text{-}out = (SI_{parenchymal} - SI_{arterial}) / SI_{arterial} \times 100$$

A subsequent wash-out value was obtained between the arterial and excretory phases by substituting $SI_{excretory}$ (signal intensity in the excretory phase) for $SI_{parenchyma}$ in the equation.

Statistical analyis

All demographic data, tumor diameters, pathologic data, MRI findings and signal intensities, of the tumor scar, cortex, aorta and noise, were recorded and all statistical analyses were conducted using SPSS for Windows software (ver. 18.0; IBM Inc).

Two observers separately evaluated the images and measured the parameters of interest in different sessions. Interobserver agreement between the two radiologists was assessed using Kappa analyses. Kappa values of 0.81–1.00 were considered indicative of good agreement. Statistical significance was accepted as $P < 0.05$. The mean values of the two observers for each parameter were used in the final analyses.

Distribution of variables was assessed using Student t test. Variables with asymmetric distribution were given as median values and (min–max) and evaluated by Mann-Whitney U test. Categorical data was presented as percentages and analyzed by chi-square test. In the evaluation of diagnostic accuracy, multiparametric analyses of each tumor were performed. Additionally, cutoff wash-in and wash-out values were calculated using receiver operating characteristic (ROC) curve analysis. The sensitivity and specificity (with 95% confidence intervals [CIs]) for differentiating among renal tumor types were also calculated.

Results

The study included 50 patients, 17 of whom had a diagnosis of oncocytoma and the rest (n=33) had a diagnosis of chromophobe RCC. In the oncocytoma group, there were 7 male (41.2%) and 10 female (58.8%) patients; in the chromophobe RCC group, there were 22 male (66.7%) and 11 female (33.3%) patients. The mean ages of the patients with oncocytoma and chromophobe RCC were 61.0±11.6 and 58.5±14.0 years, respectively. No statistically significant group difference was found in age or sex ($P = 0.50$ and $P = 0.080$, respectively).

Mean tumor diameter was 60.6±47.3 mm in the renal oncocytoma group and 61.7±45.9 mm in the chromophobe RCC group ($P = 0.93$). Nine renal oncocytoma (52.9%) cases and eleven chromophobe RCC (33.3%) cases had central scars. Mean scar diameters were 39.2±36.9 mm and 25.4±12.1 mm in the oncocytoma and chromophobe RCC groups, respectively. No statistically significant group difference was found for either the presence or diameter of central scars ($P = 0.18$ and $P = 0.31$, respectively). All central scars in the renal oncocytoma group were hyperintense on both T2-weighted images (fast spin-echo and fat saturated T2-weighted images). Nine central scars were hyperintense, and two were hypointense, on T2-weighted images in the chromophobe RCC group. There was also no statistically significant group difference in T2 scar intensity ($P = 0.14$). The RENAL scores were 7.7±1.7 and 8.2±2.3 in the renal oncocytoma and chromophobe RCC groups, respectively ($P = 0.39$). In the evaluation of tumor growth pattern, of the renal oncocytoma cases 15 (88.2%) were exophytic, and 2 (11.8%) were endophytic. In addition, of the chromophobe RCC cases 27 (81.8%) were exophytic, and 6 (18.2%) were endophytic. According to the evaluation of tumor signal homogeneity on both T2-weighted images, of the renal oncocytoma cases 2 (11.8%) were homogeneous, and 15 (88.2%) were heterogeneous. Among the chromophobe RCC tumors, 12 (36.4%) were homogeneous, and 21 (63.6%) were heterogeneous. Both the tumor growth pattern and tumor homogeneity showed no statistically significant group difference ($P = 0.55$ and $P = 0.060$, respectively). The fast spin-echo T2 signal intensities of tumors were compared with those of renal parenchyma: of the oncocytomas 7 (41.2%) were hyperintense and 10 (58.8%) were hypointense or isointense, while among the chromophobe RCC tumors, 3 (9.1%) were hyperintense and significantly more were hypointense or isointense (89.9%, n=30; $P = 0.007$). These results are summarized in Table 2.

Regarding the evaluation of interobserver agreement for all quantitative and qualitative measures, the Kappa values for all measurements ranged from 0.88 to 0.94. Signal intensity values of both tumors in fast spin-echo and fat saturated T2-weighted images represented a wide range. Oncocytomas were found to have significantly higher signal intensities than chromophobe RCCs in fast spin-echo T2-weighted images ($P = 0.021$). In fat saturated T2-weighted images chromophobe RCC had higher signal

Table 2. Results of qualitative MRI analysis of the tumors

	Oncocytoma	Chromophobe RCC	*P*
Mean tumor diameter (mm)	60.6±47.3	61.7±45.9	0.93[a]
Central scars, n (%)	9 (52.9)	11 (33.3)	0.18[b]
Mean scar diameter (mm)	39.2±36.9	25. 4±12.1	0.31[c]
Scar intensities*	Hyperintense: 9 (100) Hypointense: 0 (0)	Hyperintense: 9 (81.8) Hypointense: 2 (18.2)	0.14[b]
RENAL scores	7.7±1.7	8.2±2.3	0.39[c]
Tumor growth pattern	Exophytic: 15 (88.2) Endophytic: 2 (11.8)	Exophytic: 27 (81.8) Endophytic: 6 (18.2)	0.55[b]
Tumor signal homogeneity*	Homogeneous: 2 (11.8) Heterogeneous: 15 (88.2)	Homogeneous: 12 (36.4) Heterogeneous: 21 (63.6)	0.065[b]
Tumor T2 signal intensity compared to renal parenchyma**	Hyperintense: 7 (41.2) Hypo/isointense: 10 (58.8)	Hyperintense: 3 (9.1) Hypo/isointense: 30 (90.9)	0.007[b]

RCC, renal cell carcinoma; RENAL, Radius, Exophytic/endophytic properties, Nearness of tumor to the collecting system or sinus in millimeters, Anterior/posterior, Location relative to polar lines.
* Both T2-weighted images (fast spin-echo and fat saturated T2-weighted images).
** Fast spin-echo T2-weighted images.
[a]Student t test; [b]Chi-square test; [c]Mann-Whitney U test.

Table 3. Signal intensity ratios, wash-in and wash-out values for arterial, parenchymal, and excretory phases, and T2 signal intensities

	Oncocytoma	Chromophobe RCC	*P*[a]
Arterial phase signal intensity ratio (%)	62.03 (5.6-73.4)	44.8 (7.06-70.11)	0.01
Parenchymal phase signal intensity ratio (%)	64.3 (44.2-78.04)	40.05 (-10.7-77.9)	<0.001
Excretory phase signal intensity ratio (%)	64.2 (43.3-88.7)	33.7 (6.6-78.03)	<0.001
Arterial phase wash-in	163.3 (5.9-276.1)	81.3 (7.6-234.6)	0.001
Parenchymal phase wash-in	180.07 (79.2-355.4)	66.8 (12.04-353.4)	<0.001
Excretory phase wash-in	179.3 (76.3-786.3)	51.03 (7.07-355.1)	<0.001
Wash-out (parenchymal)	0.38 (-17.8-138.9)	-2.1 (-44.7-62.35)	0.20
Wash-out (excretory)	-5.2 (-27.3-220.7)	-7.6 (-41.8-62.9)	0.20
Fat-saturated signal intensity ratio (%)	107.4 (61.6-172.5)	97.1 (66.1-208.7)	0.17
Fast-spin echo T2 signal intensity ratio (%)	110.9 (73.2-182.3)	97.6 (70.0-152.6)	0.24
Fat-saturated T2 signal intensity	352 (132-1838)	774 (219-3598)	0.82
Fast-spin echo T2 signal intensity	454 (83-1720)	258.5 (127-3448)	0.021

Data are presented as median (min–max).
RCC, renal cell carcinoma.
[a]Mann-Whitney U test.

intensities than oncocytomas without statistical significance ($P = 0.82$). Signal intensity ratios were higher in oncocytomas than chromophobe RCCs. However, there was no statistically significant difference between two tumors in terms of signal intensity ratios. Concerning the evaluation of dynamic enhancement behavior, a statistically significant difference was found between the oncocytoma and chromophobe RCC groups in all phases (arterial, parenchymal, and excretory). In all phases, renal oncocytomas showed higher signal intensity ratios and wash-in values than chromophobe RCCs (Figs. 1 and 2). The T2 signal intensities, signal intensity ratios and wash-in and wash-out values, for all phases in both groups, are shown in Table 3.

The ROC curve analysis results for differentiating renal oncocytomas and chromophobe RCCs according to wash-in and wash-out values are shown in Fig. 3 and Table 4. The optimal cutoff wash-in value for arterial phase was 119, with a sensitivity of 84% and a specificity of 77%. In parenchymal phase, the optimal cutoff value was 117, again with a sensitivity and specificity of 84% and 77%, respectively. The optimal cutoff value in excretory phase was 103; here, the sensitivity was 90%, and the specificity was 83%. These results are summarized in Table 3. No statistically significant difference was found between the two tumor types in terms of the wash-out values.

Discussion

In this study, the dynamic contrast-enhanced MRI findings, enhancement ratios, and wash-in indexes showed promising results for differentiating between renal oncocytoma and chromophobe RCC. The dynamic contrast-enhanced MRI findings and quantitative analyses have prominent superiority to qualitative MRI features and the known radiologic limitations of these tumors (13, 16).

MRI is an excellent method in characterizing lesions most of the time. Recent studies including quantitative parameters derived from multiparametric MRI has demonstrated that RCC can be preoperatively estimated based on MRI signal intensities and enhancement rates (2, 12, 13). This may also apply to distinguishing oncocytoma and chromophobe RCC, which is in fact clinically more important because, while one of these entities is benign, the other is malignant. Although these two tumor types have different clinical behaviors and prognoses, in the presence of conventional diagnostic findings surgical treatment is indicated for both. If these tumors, particularly oncocytoma, are accurately diagnosed radiologically before the surgery, the treatment options may change and the patient may be assigned to follow-up after biopsy (17). Based on this, we investigated and compared the MRI features of oncocytomas and chromophobe RCCs. The differences in T2 signal intensities, contrast enhancement ratios and

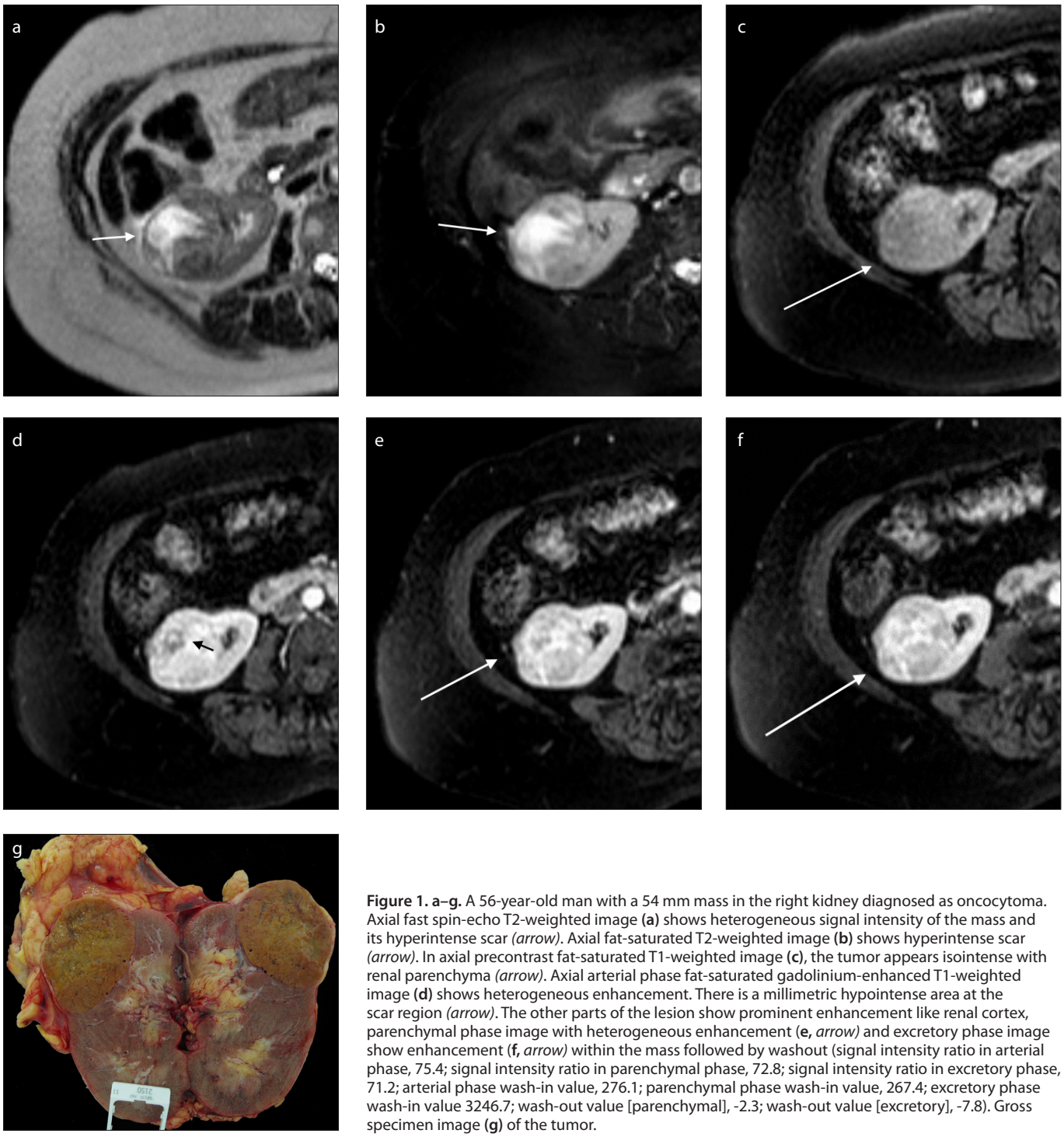

Figure 1. a–g. A 56-year-old man with a 54 mm mass in the right kidney diagnosed as oncocytoma. Axial fast spin-echo T2-weighted image **(a)** shows heterogeneous signal intensity of the mass and its hyperintense scar *(arrow)*. Axial fat-saturated T2-weighted image **(b)** shows hyperintense scar *(arrow)*. In axial precontrast fat-saturated T1-weighted image **(c)**, the tumor appears isointense with renal parenchyma *(arrow)*. Axial arterial phase fat-saturated gadolinium-enhanced T1-weighted image **(d)** shows heterogeneous enhancement. There is a millimetric hypointense area at the scar region *(arrow)*. The other parts of the lesion show prominent enhancement like renal cortex, parenchymal phase image with heterogeneous enhancement (**e,** *arrow)* and excretory phase image show enhancement (**f,** *arrow)* within the mass followed by washout (signal intensity ratio in arterial phase, 75.4; signal intensity ratio in parenchymal phase, 72.8; signal intensity ratio in excretory phase, 71.2; arterial phase wash-in value, 276.1; parenchymal phase wash-in value, 267.4; excretory phase wash-in value 3246.7; wash-out value [parenchymal], -2.3; wash-out value [excretory], -7.8). Gross specimen image **(g)** of the tumor.

wash-in values are promising with respect to reaching the correct diagnosis.

In the literature, there are limited studies on the MRI findings of oncocytoma and chromophobe RCC (12, 13). Rozenkrantz et al. (12) studied the morphologic features of these two types of tumor and concluded that both oncocytoma and chromophobe RCC have similar qualitative features on MRI and cannot be differentiated accurately. We obtained similar results regarding the morphologic MRI features of these tumors, except with respect to the T2 signal intensity ratios compared with those of the renal parenchyma. In our study, significantly more of the chromophobe RCCs were hypo- or isointense versus hyperintense (89.9% vs. 9.1%, $P = 0.007$). Regarding signal intensities measured on fast spin-echo T2-weighted images, there was a significant difference between the two tumors. This finding contrasts with that reported in the literature (13). However, there was no significant difference between the T2 signal intensity ratios of the oncocytoma and chromophobe RCC groups. Based on this result, fat-saturated tumor intensity values and T2

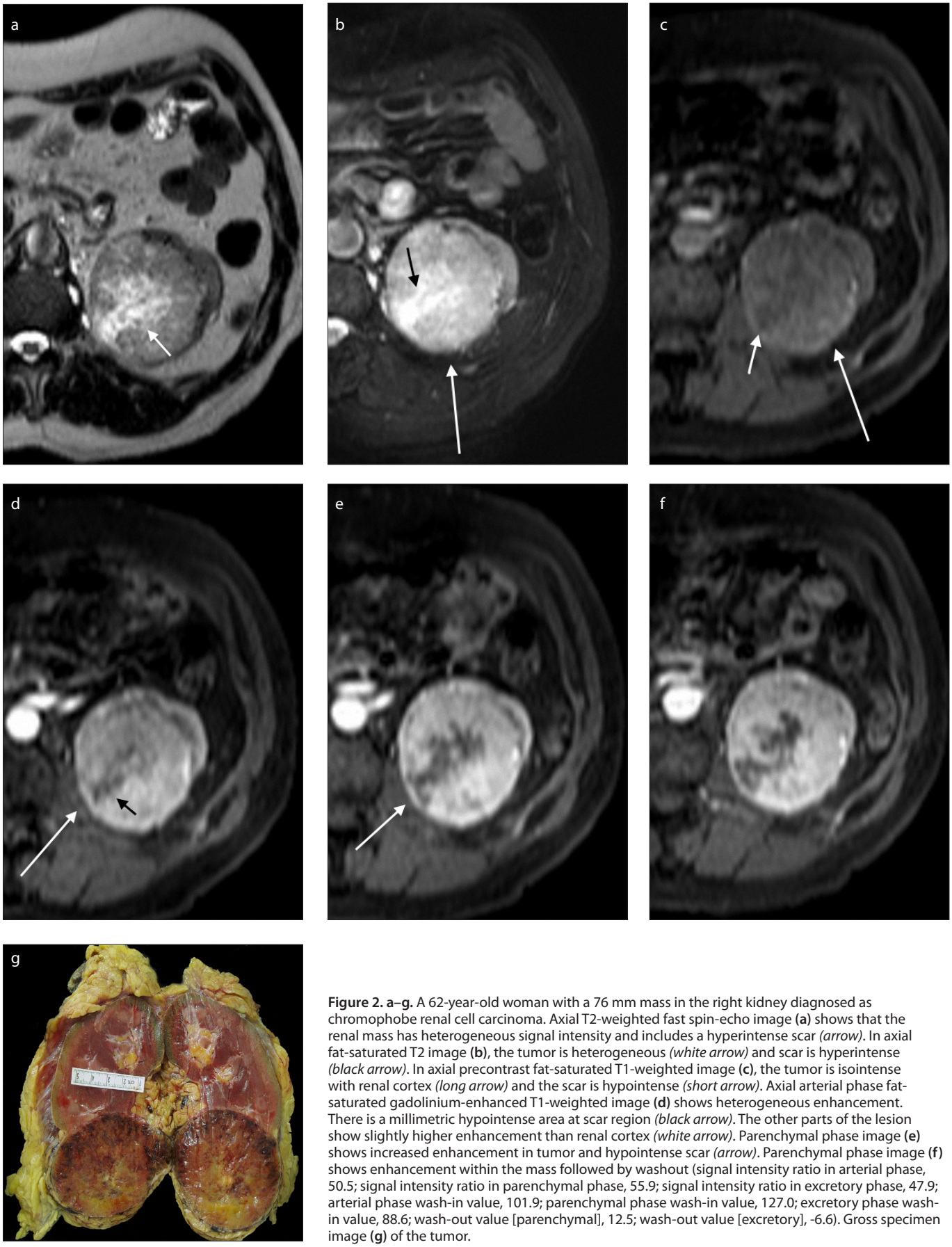

Figure 2. a–g. A 62-year-old woman with a 76 mm mass in the right kidney diagnosed as chromophobe renal cell carcinoma. Axial T2-weighted fast spin-echo image **(a)** shows that the renal mass has heterogeneous signal intensity and includes a hyperintense scar *(arrow)*. In axial fat-saturated T2 image **(b)**, the tumor is heterogeneous *(white arrow)* and scar is hyperintense *(black arrow)*. In axial precontrast fat-saturated T1-weighted image **(c)**, the tumor is isointense with renal cortex *(long arrow)* and the scar is hypointense *(short arrow)*. Axial arterial phase fat-saturated gadolinium-enhanced T1-weighted image **(d)** shows heterogeneous enhancement. There is a millimetric hypointense area at scar region *(black arrow)*. The other parts of the lesion show slightly higher enhancement than renal cortex *(white arrow)*. Parenchymal phase image **(e)** shows increased enhancement in tumor and hypointense scar *(arrow)*. Parenchymal phase image **(f)** shows enhancement within the mass followed by washout (signal intensity ratio in arterial phase, 50.5; signal intensity ratio in parenchymal phase, 55.9; signal intensity ratio in excretory phase, 47.9; arterial phase wash-in value, 101.9; parenchymal phase wash-in value, 127.0; excretory phase wash-in value, 88.6; wash-out value [parenchymal], 12.5; wash-out value [excretory], -6.6). Gross specimen image **(g)** of the tumor.

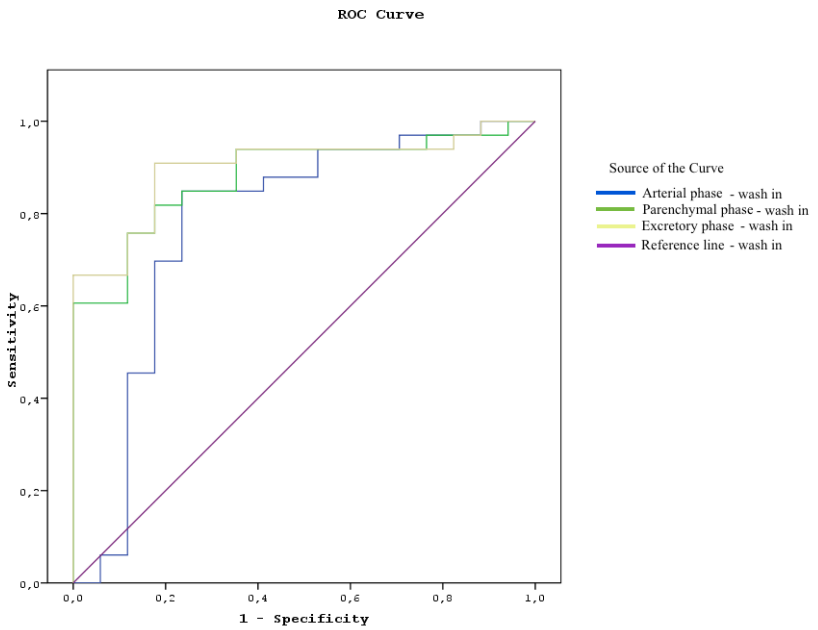

Figure 3. Receiver operating characteristic (ROC) curve of wash-in values: *blue line* denotes the arterial phase, *green line* denotes the parenchymal phase, and *yellow line* denotes the excretory phase.

Table 4. Results of ROC curve analysis

		95% confidence interval		
Wash-in values	AUC	Lower bound	Upper bound	*P*
Arterial phase	0.779	0.621	0.937	0.001
Parenchymal phase	0.881	0.786	0.975	<0.001
Excretory phase	0.900	0.813	0.987	<0.001

ROC, receiver operator characteristic; AUC, area under the curve; CI, confidence interval.

signal intensity ratios were not statistically significant in quantitative evaluations. The lack of significant difference between the T2-weighted signal intensity ratios of the oncocytoma and chromophobe RCC groups was compatible with the study of Galmiche et al. (13). Nevertheless, it may be advisable to confirm this in studies including larger series of patients.

Renal oncocytomas have been described as homogeneously enhancing, circumscribed, and well-defined masses (18, 19). Chromophobe RCCs appear as well-circumscribed, large lesions with heterogeneous enhancement (20). Despite being uncommon, necrosis and hemorrhage sites can be detected in chromophobe RCCs (20). Unlike chromophobe RCCs, oncocytomas do not contain sites of necrosis or hemorrhage (21). Both tumors are rarely characterized by cystic changes (20). In our study, 2 (11.8%) of the renal oncocytoma cases were homogeneous, and 15 (88.2%) were heterogeneous. Among the chromophobe RCC tumors, 12 (36.4%) were homogeneous, and 21 (63.6%) were heterogeneous. This result is different from the literature, probably due to variance of the sample group among the studies. Central stellate scars are characteristic of renal oncocytomas, but they are not a diagnostic feature (22). Chromophobe RCCs may also include central scars (23); in our study, 52.9% of the oncocytoma cases, and 33.3% of the chromophobe RCCs, had central scars, which were not considered a discriminating feature.

There are a few studies that have evaluated the enhancement patterns of renal RCCs (13, 24–28). In a study conducted by Lee-Felker et al. (25), on multiphasic CT, chromophobe had significantly lower maximum attenuation values than clear-cell RCCs in parenchymal and excretory phases. However, in another study, chromophobe RCCs showed higher maximum attenuation values in arterial phase versus phase 2 (24). According to the MRI enhancement patterns, changes in tumor signal intensity were moderate for chromophobe RCC in arterial and parenchymal phases (24). In a multiparametric MRI study by Galmiche et al. (13), the enhancement pattern of renal oncocytomas and chromophobe RCCs were investigated using quantitative parameters in 16 renal oncocytomas and 7 chromophobe RCCs. In that study, tumor types showed slightly different enhancement patterns on dynamic contrast-enhanced images. Another study including 16 renal oncocytomas and 32 chromophobe RCCs concluded that in three postcontrast phases %SI was higher in renal oncocytoma than chromophobe RCC (28). In our study, oncocytomas had 52%–62% enhancement ratios after administration of contrast material, while chromophobe RCCs had 37%–41% ratios; the ratios also varied by phase. The contrast enhancement ratios and wash-in values of the tumors in our study showed statistically significant differences among phases. Wash-in values of oncocytoma in the excretory phase demonstrated significant differences to other phases in multivariate analysis, and hence may be helpful for differentiating between renal oncocytoma and chromophobe RCC. In a previous study, chromophobe RCCs had slower and lower wash-in values than oncocytomas and there was a statistically significant difference in the wash-in values between arterial and parenchymal phases, allowing discrimination between the tumor types. In excretory phase, there was borderline significance (13). However, the differences between the wash-in index values were higher, the wash-in values of oncocytomas were almost double those of the wash-in values of the chromophobe RCCs. In our study, when comparing with chromophobe RCCs, wash-in index values in all phases showed a statistically significant difference for the diagnosis of oncocytoma. Similar to a previous study (13), the wash-out indexes of tumors showed no statistically significant difference in our study. The number of patients with chromophobe RCCs (n=33) and quantitative data in our study was higher than that in

that previous study (n=7), (13) possibly explaining the difference in results.

In our study, the mean RENAL score of the renal oncocytoma group was 7.7±1.7 and that of the chromophobe RCC group was 8.2±2.3. Although our study is the first to evaluate the RENAL nephrometry scores for both renal oncocytomas and chromophobe RCCs, no statistically significant difference in these scores was found between the groups. Recently, RENAL nephrometry score was proposed for evaluation of renal mass complexity and standardization of anatomical descriptions, to facilitate the decision for nephron-sparing surgery (29). The rationale involving RENAL nephrometry score evaluation in this study was to obtain data about the growing behavior of these two tumors and to investigate the possibility of a parameter that can be used. However, the obtained results were not promising.

In characterization and discrimination of benign and malignant renal masses, ^{99m}Tc-MIBI SPECT/CT scintigraphy is one of the leading imaging methods (30, 31). ^{99m}Tc-MIBI uptake is a marker of mitochondrial metabolism and is useful in imaging renal masses with rich mitochondrial content such as renal oncocytoma. Preoperative ^{99m}Tc-MIBI planar imaging may play a role in diagnosis of renal oncocytoma (31, 32). However, MRI with multiplanar imaging capability, excellent contrast resolution, and the lack of ionizing radiation may also be a promising tool in differentiation of oncocytoma and chromophobe RCC.

Our study has some limitations. First, it was a retrospective study and, as such, might include selection bias since the final diagnoses were known. However, the radiologists were blinded during the measurements to minimize this bias. Second, although we collected data from three institutions, the number of patients was still relatively low, particularly the number of oncocytoma cases. However, compared with other MRI studies reported in the literature, our sample size can be considered above average (12, 13). Third, as this retrospective series was conducted over a long period, we were limited in terms of obtaining a complete series of all MRI sequences; this not only reduced the number of patients included but also restricted the use of more recent MRI techniques, such as diffusion-weighted imaging and derived mathematical methods (33). In other words, the long-term retrospective design, limited the multiparametric nature of the study.

In conclusion, signal intensity ratios measured in dynamic contrast-enhanced MRI sequences constitute a radiologic diagnostic criterion for discriminating between renal oncocytomas and chromophobe RCCs. In this study, oncocytomas had higher signal intensity values than chromophobe RCCs in all postcontrast phases. The wash-in values of both tumors are also very useful for distinguishing renal oncocytomas from chromophobe RCCs. A high wash-in value strongly indicates a diagnosis of renal oncocytoma. As morphologic MRI features cannot be used to distinguish these two types of tumor, and because the treatment options for these tumors are different, dynamic MRI sequences and signal intensity measurements could facilitate correct diagnosis and management. To improve the diagnostic utility of dynamic MRI and achieve definitive results, more studies including larger numbers of patients and additional MRI techniques and measurements are needed.

Conflict of interest disclosure

The authors declared no conflicts of interest.

References

1. Moch H, Cubilla AL, Humphrey PA, Reuter VE, Ulbright TM. The 2016 WHO classification of tumours of the urinary system and male genital organs- part a: renal, penile, and testicular tumours. Eur Urol 2016; 70:93–105. [CrossRef]
2. Cornelis F, Tricaud E, Lasserre AS, et al. Routinely performed multiparametric magnetic resonance imaging helps to differentiate common subtypes of renal tumours. Eur Radiol 2014; 24:1068–1080. [CrossRef]
3. Sasiwimonphan K, Takahashi N, Leibovich BC, et al. Small (<4 cm) renal mass: differentiation of angiomyolipoma without visible fat from renal cell carcinoma utilizing MR imaging. Radiology 2012; 263:160–168. [CrossRef]
4. Eble JN, Sauter G, Epstein JI, Sesterhenn IA. World Health Organization classification of tumours. Pathology and genetics of tumours of the urinary system and male genital organs. Lyon: IARC Press, 2004.
5. Amin MB, Paner GP, Alvarado-Cabrero I, et al. Chromophobe renal cell carcinoma: histomorphologic characteristics and evaluation of conventional pathologic prognostic parameters in 145 cases. Am J Surg Pathol 2008; 32:1822–1834. [CrossRef]
6. Cornelis F, Lasserre AS, Tourdias T, et al. Combined late gadolinium-enhanced and double-echo chemical-shift MRI help to differentiate renal oncocytomas with high central T2 signal intensity from renal cell carcinomas. AJR Am J Roentgenol 2013; 200:830–838. [CrossRef]
7. Gakis G, Kramer U, Schilling D, et al. Small renal oncocytomas: differentiation with multiphase CT. Eur J Radiol 2011; 80:274–278. [CrossRef]
8. Chen F, Gulati M, Hwang D, et al. Voxel-based whole-lesion enhancement parameters: a study of its clinical value in differentiating clear cell renal cell carcinoma from renal oncocytoma. Abdom Radiol 2017; 42:552–560. [CrossRef]
9. Cheville JC, Lohse CM, Zincke H, Weaver AL, Blute ML. Comparisons of outcome and prognostic features among histologic subtypes of renal cell carcinoma. Am J Surg Pathol 2003; 27:612–624. [CrossRef]
10. Tikkakoski T, Paivansalo M, Alanen A, et al. Radiologic findings in renal oncocytoma. Acta Radiol 1991; 32:363–367. [CrossRef]
11. Quinn MJ, Hartman DS, Friedman AC, et al. Renal oncocytoma: new observations. Radiology 1984; 153:49–53. [CrossRef]
12. Rosenkrantz AB, Hindman N, Fitzgerald EF, et al. MRI features of renal oncocytoma and chromophobe renal cell carcinoma. AJR Am J Roentgenol 2010; 195:421–427. [CrossRef]
13. Galmiche C, Bernhard JC, Yacoub M, et al. Is multiparametric MRI useful for differentiating oncocytomas from chromophobe renal cell carcinomas? AJR Am J Roentgenol 2017; 208:343–350. [CrossRef]
14. Williamson SR, Gadde R, Trpkov K, et al. Diagnostic criteria for oncocytic renal neoplasms: a survey of urologic pathologists. Hum Pathol 2017; 63:149–156. [CrossRef]
15. Vilaseca RM, Westphalen AC, Reis HF, et al. Reproducibility and interobserver agreement of the R.E.N.A.L. nephrometry score: focus on imaging features. Radiol Bras 2017; 50:7–12. [CrossRef]
16. Harmon WJ, King BF, Lieber MM. Renal oncocytoma: magnetic resonance imaging characteristics. J Urol 1996; 155:863–867. [CrossRef]
17. Algorithm of Clinical Management of Clinical T1 Renal Mass. https://www.auanet.org/common/pdf/education/clinical-guidance/Renal-Mass-Algorithm 2009.
18. Garant M, Bonaldi VM, Taourel P, et al. Enhancement patterns of renal masses during multiphase CT acquisitions. Abdom Imaging 1998; 23:431–436. [CrossRef]
19. Zeman RK, Zeiberg A, Hayes WS, et al. Helical CT of renal masses: the value of delayed scans. AJR Am J Roentgenol 1996; 167:771–776. [CrossRef]
20. Gurel S, Narra V, Elsayes KM, et al. Subtypes of renal cell carcinoma: MRI and pathological features. Diagn Interv Radiol 2013; 19: 304–311. [CrossRef]
21. Zhang J, Lefkowitz RA, Ishill NM, et al. Solid renal cortical tumors: differentiation with CT. Radiology 2007; 244:494–504. [CrossRef]
22. Cochand-Priollet B, Molinie V, Bougaran J, et al. Renal chromophobe cell carcinoma and oncocytoma: a comparative morphologic, histochemical, and immunohistochemical study of 124 cases. Arch Pathol Lab Med 1997; 121:1081–1086.
23. Ren A, Cai F, Shang YN, et al. Differentiation of renal oncocytoma and renal clear cell carcinoma using relative CT enhancement ratio. Chin Med J 2015; 128: 175–179. [CrossRef]
24. Young JR, Margolis D, Sauk S, et al. Clear cell renal cell carcinoma: discrimination from other renal cell carcinoma subtypes and oncocytoma at multiphasic multidetector CT. Radiology 2013; 267:444–453. [CrossRef]

25. Lee-Felker SA, Felker ER, Tan N, et al. Qualitative and quantitative MDCT features for differentiating clear cell renal cell carcinoma from other solid renal cortical masses. AJR Am J Roentgenol 2014; 203:516–524. [CrossRef]
26. Sun MR, Ngo L, Genega EM, et al. Renal cell carcinoma: dynamic contrast-enhanced MR imaging for differentiation of tumor subtypes—correlation with pathologic findings. Radiology 2009; 250: 793–802. [CrossRef]
27. Young JR, Coy H, Kim HJ et. al. Performance of relative enhancement on multiphasic MRI for the differentiation of clear cell carcinoma (RCC) from papillary and chromophobe RCC subtypes and oncocytoma. AJR Am J Roentgenol 2017; 208:812–819. [CrossRef]
28. Zhong Y, Wang H, Shen Y et. al. Diffusion-weighted versus-contrast enhanced MR imaging for the differentiation or renal oncocytoma and chromophobe renal cell carcinomas. Eur Radiol 2017; 27:4913–4922. [CrossRef]
29. Kutikov A, Uzzo RG. The R.E.N.A.L. nephrometry score: a comprehensive standardized system for quantitating renal tumor size, location and depth. J Urol 2009;182:844–853. [CrossRef]
30. Campbell SC, Novick AC, Belldegrun A, et al. Guideline for management of the clinical T1 renal mass. J Urol 2009;182:1271–1279. [CrossRef]
31. Sheikhbahaei S, CS, MD, Porter KK et. al. Defining the added value of 99mTc-MIBI SPECT/CT to conventional cross-sectional imaging in the characterization of enhancing solid renal masses. Clin Nucl Med 2017; 42:188–193. [CrossRef]
32. Gormley TS, Van Every MJ, Moreno AJ. Renal oncocytoma: preoperative diagnosis using technetium 99m sestamibi imaging. Urology 1996; 48:33–39. [CrossRef]
33. Shen L, Zhou L, Liu X, Yang X. Comparison of biexponential and monoexponential DWI in evaluation of Fuhrman grading of clear cell renal cell carcinoma. Diagn Interv Radiol 2017; 23:100–105. [CrossRef]